

Please cite this article in press as: Mohanty JR et al., Evaluation of overload-induced fatigue crack growth ..., Engng Fract Mech (2008),

<http://dx.doi.org/10.1016/j.engfracmech.2008.03.001>

archived in Dspace@nitr

<http://dspace.nitrkl.ac.in/dspace>

Evaluation of overload-induced fatigue crack growth retardation parameters using an exponential model

J.R. Mohanty^a, B.B. Verma^a, P.K. Ray^{b,*}

^a *Department of Metallurgical and Materials Engineering, National Institute of Technology, Rourkela 769 008, India*

^b *Department of Mechanical Engineering, National Institute of Technology, Rourkela 769 008, India*

Abstract

In this study, fatigue crack growth rate in mixed-mode overload (modes I and II) induced retardation zone has been predicted by using an “Exponential model”. The important parameter of this model is the specific growth rate. This has been correlated with various crack driving parameters such as stress intensity factor range, maximum stress intensity factor, equivalent stress intensity factor, and mode mixity, as well as material properties such as modulus of elasticity and yield stress. An equation has been formulated for specific growth rate which has been used to calculate crack growth rate under mixed-mode loading conditions. It has been observed that the crack growth rate predicted by the model is in good agreement with experimental results.

Keywords: Delay cycle; Exponential model; Fatigue crack growth retardation; Retarded crack length; Retardation parameters

1. Introduction

Prediction of life of a structural or a machine component is a challenging job for the engineering community. Because of high cost of critical components, they should be used for optimum life and be replaced only before a shutdown or failure is due. Also it is important to know the life of a critical component so that it can be replaced before a catastrophic failure occurs. Fatigue crack propagation under service loading condition generally involves variable amplitude rather than constant amplitude loading. During the growth of a fatigue crack, load excursion in the form of a single tensile overload may occur either in normal-mode or in mixed-mode due to alteration of loading direction or the orientation of the crack or defect. It is known that a single tensile overload retards a growing fatigue crack and thereby the life of the component is increased. However, the application of fracture mechanics to predict the life of a component, especially when there is mixed-mode

* Corresponding author. Tel.: +91 661 2462518.

E-mail addresses: prabal_kray@yahoo.com, pkray@nitrrkl.ac.in (P.K. Ray).

Nomenclature

a, a_d, a_0	crack length: in general, retarded and initial
A', B'	curve fitting constants in the 'Exponential Model'
B	specimen thickness
E	Young's modulus
F	applied load
$f(g)$	geometrical factor in stress intensity factor (SIF) expression
$K_I, K_{II}, \Delta K$	stress intensity factor: mode I, mode II and range
K_I^{ol}, K_{II}^{ol}	stress intensity factor at overload: in mode I and mode II
K_{eq}^{ol}	equivalent stress intensity factor
K_{max}^B	maximum baseline stress intensity factor
l	a parameter to correlate different crack driving parameters with specific growth rate
m	specific growth rate parameter
N, N_d	load cycle number: in general and delay
P_0, P_t	population: initial and at any time ' t '
r	Malthusian parameter/population growth rate
R^{ol}	overload ratio
w	specimen width
α_1	ratio of mode I and mode II fracture toughness
β	loading angle
σ_{ys}	yield stress

load-interaction in crack growth, is still in the developing stage due to the inability to generalize and translate laboratory data to real life situations. Mixed-mode overloads are common in case of turbine shafts, railway tracks, angled cracks in pressure vessels and pressure cabins and in many welds.

Most of the literature is concerned with mode I overload leading to extensive retardation effect which enhances the residual life of a structure. Iida and Kobayashi [1] were the first to study the mixed-mode (I & II) problem. Later Forman et al., [2], Roberts and Kibler [3], Tanaka [4], Sih [5,6], Tanaka [4], Patel and Pandey [7] gave more insight to mixed-mode crack problems. Srinivas and Vasudevan [8], Sander and Richard [9,10] worked on mixed-mode (I and II) overloads. Srinivas and Vasudevan [8] gave physical interpretation of mixed-mode overload through fractographic studies. Sander and Richard [9] did finite element analysis of fatigue crack growth for mixed-mode overloads. Later they carried out experimental investigations in order to explain the overload-induced retardation [10]. Munro [11] enumerated data smoothing technique to obtain fatigue crack growth rate. Smith [12] determined fatigue crack growth from experimental data. Sudip and Kujawski [13] correlated R -ratio effects with FCGR. Sadananda and Vasudevan [14] established, in addition to ΔK , the role of K_{max} in fatigue crack growth problems. This method is known as two parameter method or unified approach. Later, Zhang et al. [15] used a new parameter defined by crack extension due to change of applied stress, and proved the two loading parameters are necessary in order to accurately describe fatigue crack propagation rate. However, a quantitative relationship among FCGR and the crack driving parameters was lacking. In the present work the authors have attempted to achieve this by using an Exponential model. The Exponential model is quite often used for calculation of growth of population/bacteria etc. The basic equation of the above model is

$$P_t = P_0 e^{rt} \quad (1)$$

For prediction of crack growth the above equation is rewritten as

$$a = a_0 e^{mN} \quad (2)$$

When the above model is used and tested in the present study, it is observed that the results obtained by the above model are in good agreement with the experimental results.

2. Experimental

This study was conducted using 7020 Al-alloy (used for ground transport system) procured from Hindalco, Renukoot, India, in the as-fabricated condition. The alloy was subjected to T7 heat-treatment comprising solution treatment, quenching and two-stage ageing at 110 °C for 8 h followed by 150 °C for 18 h to obtain optimum properties. The chemical composition and the mechanical properties of the alloy are given in Tables 1 and 2, respectively.

Single-edge notched tension, SEN(T) specimens having a thickness of 6.5 mm were used for conducting the fatigue test. The specimens were made in the longitudinal transverse (LT) direction from the plate. The detail geometry of the specimens is given in Fig. 1.

The experiments were performed in *Instron*-8502 machine with 250 kN load cell, interfaced to a computer for machine control and data acquisition. All tests were conducted in air and at room temperature. The test specimens were fatigue pre-cracked under mode I loading to an a/w ratio of 0.3 and were subjected to constant load test (i.e. progressive increase in ΔK with crack extension) maintaining a load ratio of 0.1. The sinusoidal

Table 1
Composition of the material

Element	Cu	Mg	Mn	Fe	Si	Zn	Al
Wt.%	0.05	1.20	0.43	0.37	0.22	4.60	Balance

Table 2
Mechanical properties of specimen material

Tensile strength (σ_{ut})	352.14 MPa
Yield strength (σ_{ys})	314.7 MPa
Young's modulus (E)	70,000 MPa
Elongation in 40 mm	21.54%

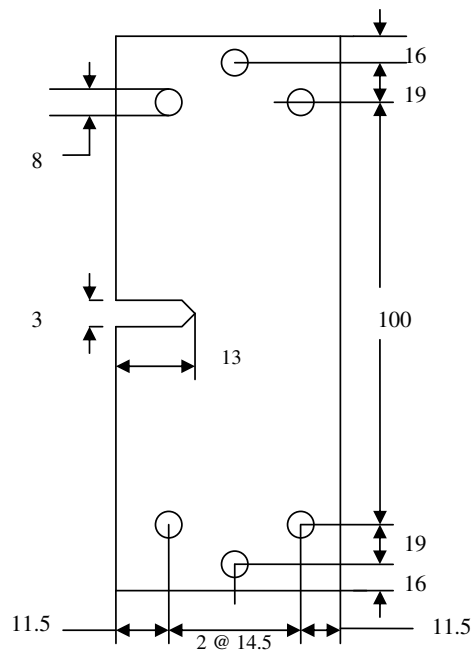


Fig. 1. Single-edge notch tension (SENT) Specimen geometry.

loads were applied at a frequency of 6 Hz. The crack growth was monitored with the help of a COD gauge mounted on the face of the machined notch. The fatigue crack was allowed to grow up to an a/w ratio of 0.4 and subsequently subjected to single overload spike at a loading rate of 8 kN/min.

The overloading was done by using the mixed-mode loading device shown in Fig. 2, which is similar to the one used by Richard [16]. The following equations are used to determine stress intensity factors K_I and K_{II} for different angles of overload application,

$$K_I = f(g) \cdot \frac{F \cos \beta \cdot \sqrt{\pi a}}{wB} \quad (3)$$

$$K_{II} = f(g) \cdot \frac{F \sin \beta \cdot \sqrt{\pi a}}{wB} \quad (4)$$

where

$$f(g) = 1.12 - 0.231(a/w) + 10.55(a/w)^2 - 21.72(a/w)^3 + 30.39(a/w)^4 \quad (5)$$

The specimens were subjected to mode I, mode II, and mixed-mode overloads at different loading angles, β ($=18^\circ, 36^\circ, 54^\circ$ and 72°) and overload ratios, R^{ol} ($=2.5, 2.6, 2.7$ and 2.8). The overload ratio is defined as

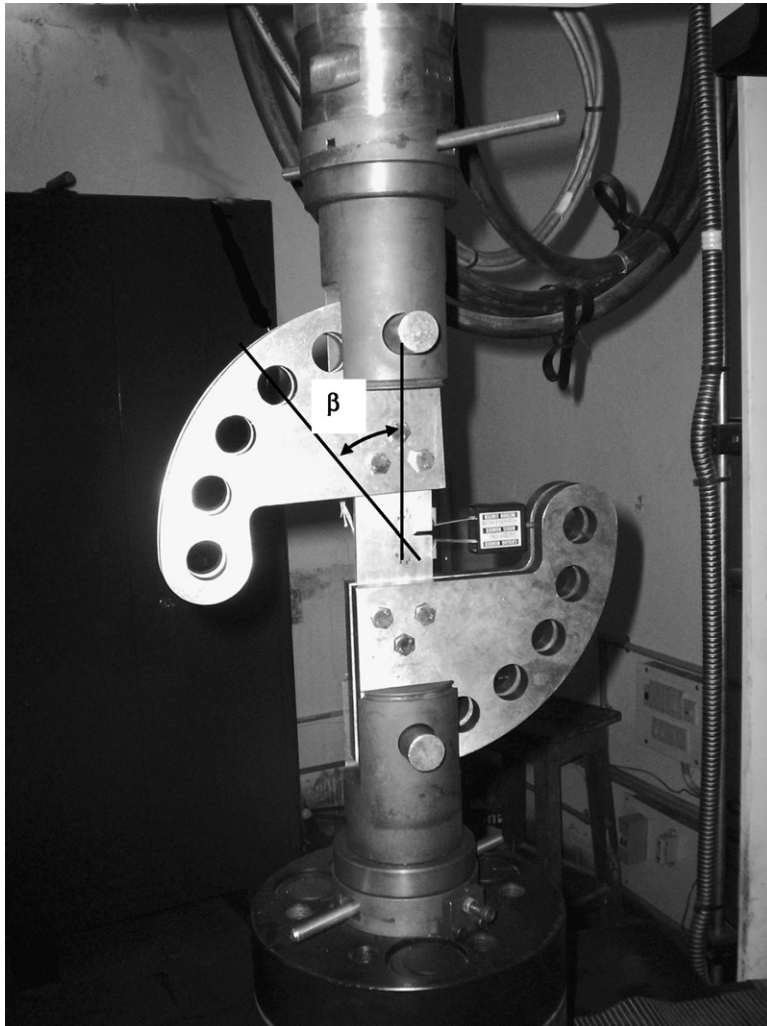


Fig. 2. Mixed-mode loading fixture.

$$R^{ol} = \frac{K_{eq}^{ol}}{K_{max}^B} \quad (6)$$

where K_{max}^B is the maximum stress intensity factor for base line test. The equivalent stress intensity factor K_{eq}^{ol} is calculated according to the following equation [13]:

$$K_{eq}^{ol} = 0.5K_I^{ol} + 0.5\sqrt{(K_I^{ol})^2 + 4(\alpha_1 K_{II}^{ol})^2} \quad (7)$$

where $\alpha_1 = (K_{IC}/K_{IIc}) = 0.95$ according to strain energy density theory [17] and K_I^{ol} and K_{II}^{ol} are the fractions of stress intensity factors of modes I and II during the overload, respectively. Then the fatigue test was continued in mode I.

3. Results and discussion

3.1. Modeling

The differential equation describing an exponential growth is

$$\frac{dP}{dt} = rP \quad (8)$$

where P is population and t is time.

The solution of the above differential equation is

$$P(t) = P_0 \cdot e^{rt} \quad (9)$$

This equation is called the law of growth, and the quantity r in this equation is sometimes referred to as the Malthusian parameter, also known as specific growth rate.

When $t = 0$, $P = P_0$. However, as $t \rightarrow \infty$, P also tends to infinity. But at any point of time the population cannot become infinite due to natural calamities like flood, famine etc. So some modification is required if this model is to be used for calculation of growth of population.

However, in the present case, a crack will grow infinitely (of course the plate width has to be infinite) as $t \rightarrow \infty$. Therefore, the equation without any modification is acceptable for fatigue crack growth studies and the basic equation used here is

$$a = a_0 e^{mN} \quad \text{or} \quad m = \frac{\ln(a/a_0)}{N} \quad (10)$$

The values of m can be calculated from crack extension and number of load cycles data. The $a-N$ curves for various overload conditions are presented in Fig. 3.

The important parameter in the model is the specific growth rate m . This is correlated with different crack driving parameters such as K_{max} , K_{eq}^{ol} and ΔK , as well as the material properties E and σ_{ys} , and is defined by the equation

$$m = A' l + B' \quad \text{where} \quad l = \left[\frac{K_{eq}^{ol}}{K_{max}} \right] \times \left[\frac{K_{eq}^{ol}}{\Delta K} \right] \times \left[\frac{E}{\sigma_{ys}} \right] \quad (11)$$

The variations of m with l for various overload angles are given in Fig. 4. It is observed that these variations are linear. However, the constants of the equations (slope and intercept) are different for each overload angle. Hence, these are correlated with the overload angles represented by the factor $\frac{K_{II}}{K_I + K_{II}}$ [10] and the values are given in the following equations:

$$A' = \left[-2.8511 \times \left(\frac{K_{II}}{K_I + K_{II}} \right) - 1.727 \right] \times 10^{-9} \quad (12)$$

$$\text{and} \quad B' = \left[-53.79 \times \left(\frac{K_{II}}{K_I + K_{II}} \right)^2 + 99.152 \times \left(\frac{K_{II}}{K_I + K_{II}} \right) + 24.313 \right] \times 10^{-7} \quad (13)$$

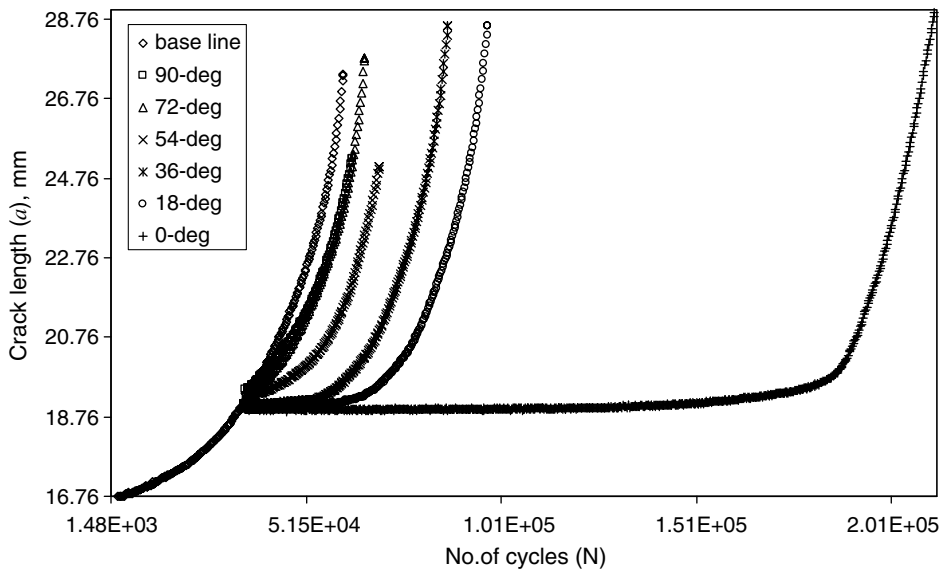


Fig. 3. a - N curves for all the angles of overload.

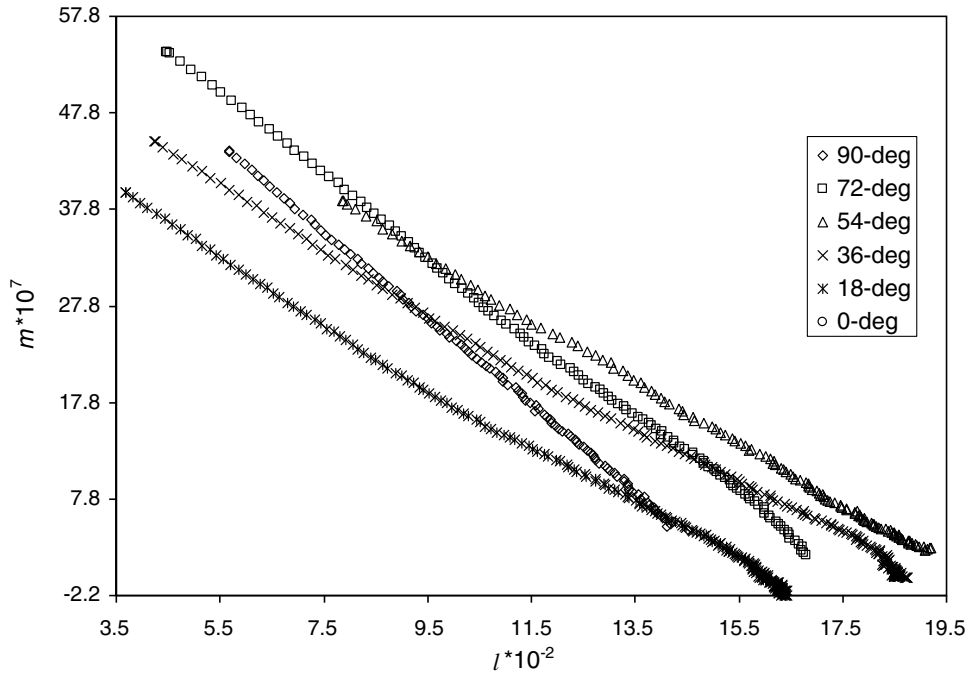


Fig. 4. Variation of m with l .

While developing the above equation all the experimental data have been considered except data for mixed-mode case having $\beta = 54^\circ$, which has been predicted from the model and tested with experimental data.

3.2. Significance of specific crack growth rate (m)

As discussed earlier, m is an important parameter in the above model for fatigue crack growth. It may be noted that m is not a constant quantity. It changes with change in loading condition as well as crack length.

Since in constant load fatigue test, crack length increases with number of cycles resulting increase in stress intensity factor, m also changes with crack length and number of cycles. The typical variation of m with crack length and number of cycles are shown in Figs. 5 and 6, respectively. Sadananda and Vasudevan [14] observed

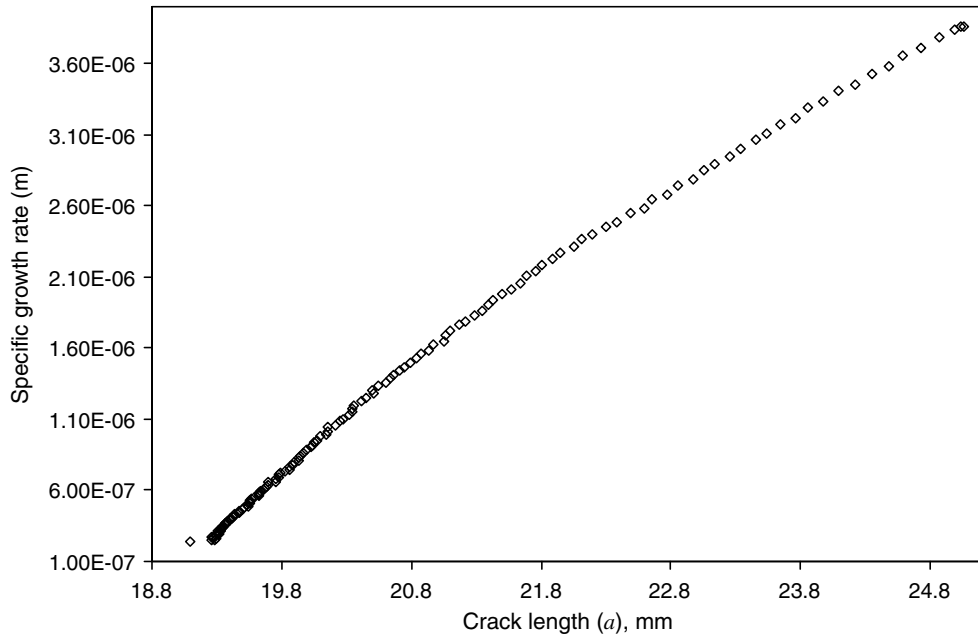


Fig. 5. Variation of specific growth rate (m) with crack length (a) for overload angle 54° .

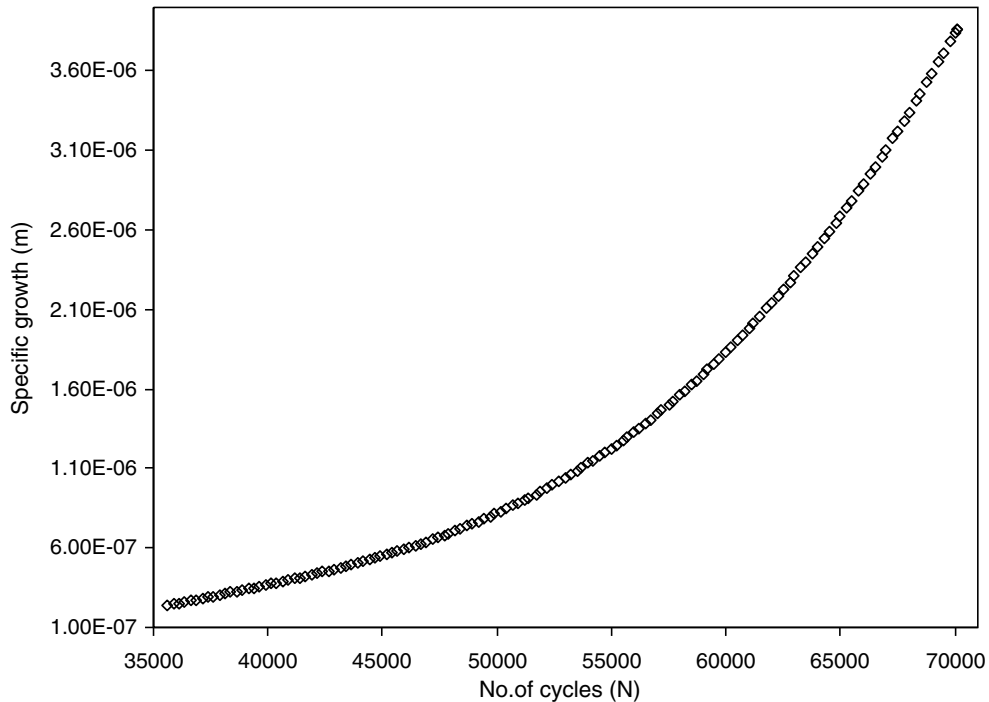


Fig. 6. Variation of specific growth rate (m) with number of cycles (N) for overload angle 54° .

that fatigue crack growth is not only dependent on ΔK but also on K_{\max} . Therefore, m will depend on both ΔK and K_{\max} as long as there is no load-interaction. Since we are concerned with mixed-mode overload cases, m will also depend on the overload-induced monotonic plastic zone. When the crack is inside this plastic zone, the nature of growth of m will be different from that when the crack is outside of this zone. Therefore, to take into account the load-interaction effect the factor $K_{\text{eq}}^{\text{ol}}$ has been introduced. Further, m is also influenced by the two material properties E and σ_{ys} . Hence, the dependence of m on these parameters is represented through the dimensionless groups $(K_{\text{eq}}^{\text{ol}}/K_{\max})$, $(K_{\text{eq}}^{\text{ol}}/\Delta K)$, and (E/σ_{ys}) , and have been introduced in Eq. (11). Finally the

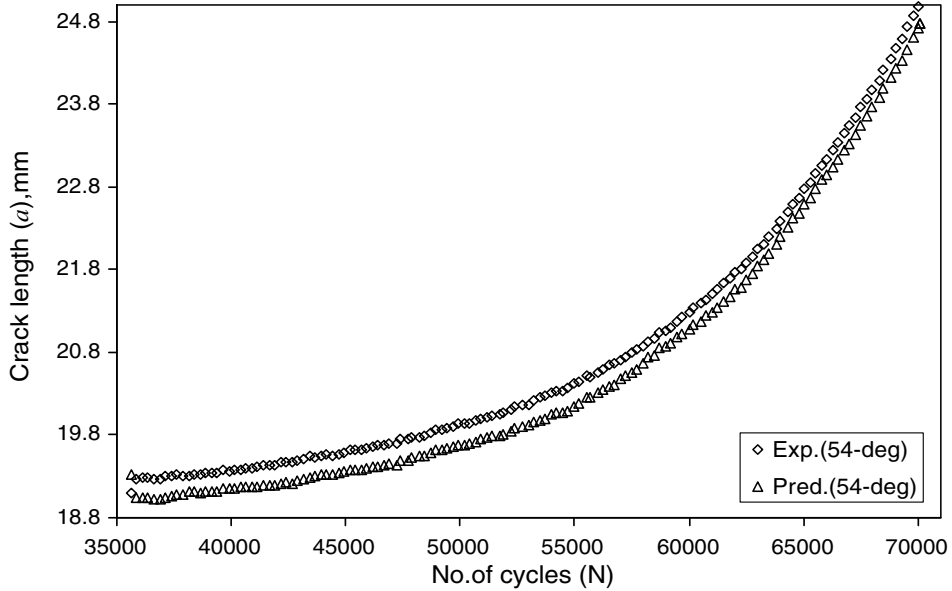


Fig. 7. Comparison of experimental and predicted a - N curves for 54° overload angle.

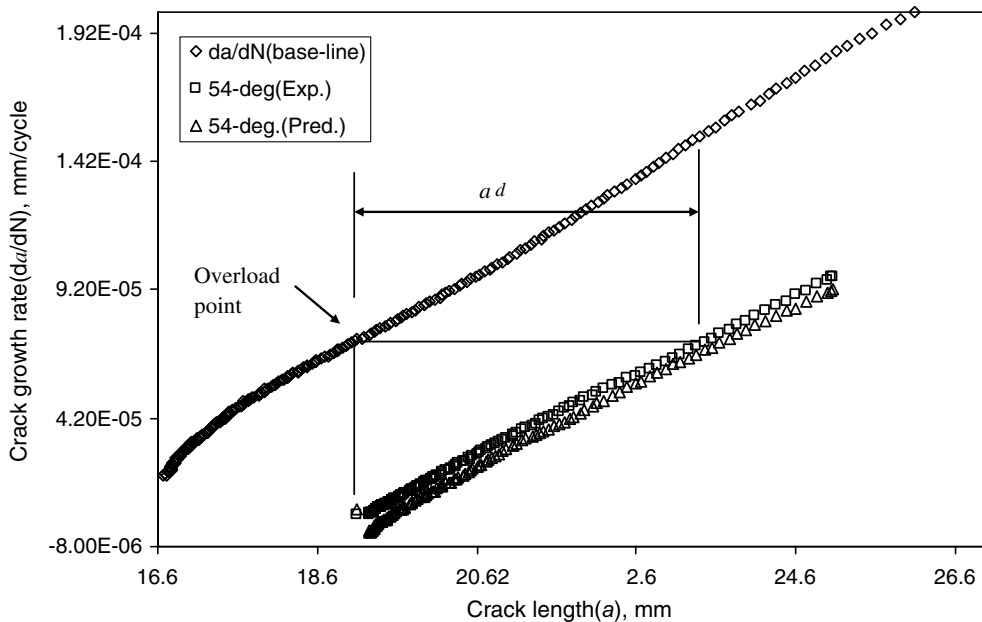


Fig. 8. Comparison of predicted and experimentally obtained retarded crack length (a_d) for overload angle 54° .

factor $(K_{II}/K_I + K_{II})$ is introduced in the equation of m in order to account for mode I, mode II, and mixed-mode (I and II) load-interaction effect.

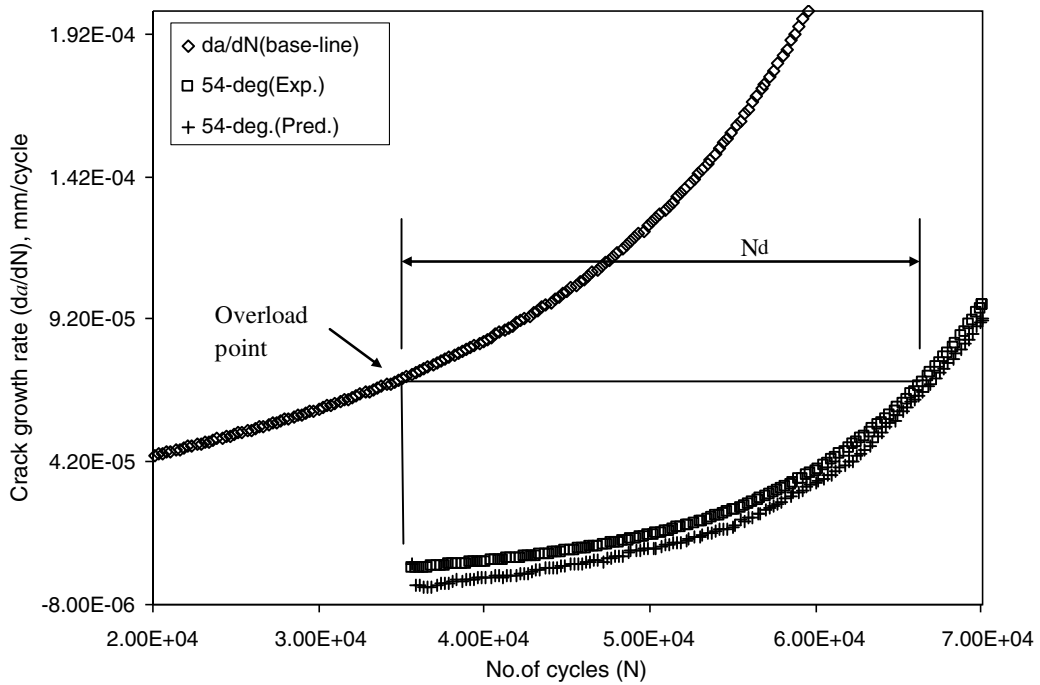


Fig. 9. Comparison of predicted and experimentally obtained delay cycles (N_d) for overload angle 54° .

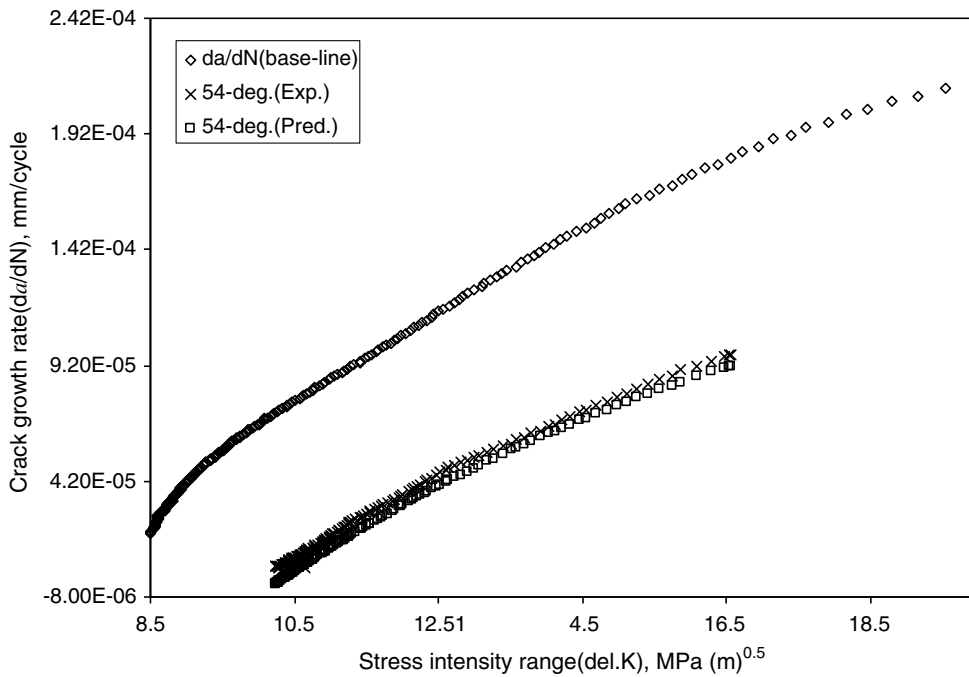


Fig. 10. Comparison of experimental and predicted crack growth rate (da/dN) for overload angle 54° .

Table 3

Retarded crack length (a_d) and delay cycle (N_d) at various overload angles

Angle (β) of overload application	Retarded crack length (a_d) (mm)	Delay cycle (N_d)
90°	3.754	22000
72°	3.784	22303
54° (exp.)	4.281	30937
54° (pred.)	4.483	31388
36°	5.01	45070
18°	5.829	57121
0°	10.843	178367

3.3. Model testing

Equations were derived by excluding data of overload angle 54° and the model has been tested by comparing experimental data of overload angle 54° with the predicted ones using the model. The results obtained are presented in Figs. 7–10. Fig. 7 shows the experimental and predicted a – N curves for overload angle 54°. Figs. 8 and 9 show the variations of crack growth rate (da/dN) with crack length (a) and number of cycles (N), respectively. The retarded crack length (a_d) and delay cycle N_d for experimental data and that for predicted value for overload angle 54° only are presented in Table 3. The percentage deviation of predicted a_d value and the one obtained from experimental data is +4.7. The percentage deviation of predicted N_d value from the experimental value is +1.458. The predicted ΔK – da/dN plot is also matching with the experimental one for overload angle 54° (Fig. 10).

4. Conclusion

1. Exponential model of the form $a = a_0 e^{mN}$ can be effectively used to determine the retardation parameters a_d and N_d .
2. The value of m increases with crack extension and number of cycles.
3. In the retardation zone the intrinsic growth rate m is a function of specimen geometry and loading parameters defined by ΔK , K_{\max} and $K_{\text{eq}}^{\text{ol}}$, mode mixity [$K_{\text{II}}/(K_{\text{I}} + K_{\text{II}})$] and material properties E and σ_{ys} .
4. The intrinsic growth rate m can be represented by an equation of the form $m = Al + B$ where $l = \left[\frac{K_{\text{eq}}^{\text{ol}}}{K_{\max}} \right] \times \left[\frac{K_{\text{eq}}^{\text{ol}}}{\Delta K} \right] \times \left[\frac{E}{\sigma_{\text{ys}}} \right]$ and A and B are functions of $\frac{K_{\text{II}}}{K_{\text{I}} + K_{\text{II}}}$.
5. Percent errors for the retardation parameters predicted by the above model are +4.7 for a_d and +1.458 for N_d .

Acknowledgements

The authors thank CSIR, India, for sponsoring this project (Project No. 22(373)/04/EMR II). They also thank Hindalco, Renukoot, India, for supplying the aluminium alloy for this research project.

References

- [1] Iida S, Kobasahi AS. Crack propagation in 7075-T6 plates under cyclic tensile and transverse shear loadings. J Basic Eng Series 1969;D91:764–9.
- [2] Forman RG, Kearney VE, Engle RM. Numerical analysis of crack propagation in a cyclic-loaded structures. J Basic Eng Series 1967;D89:459–64.
- [3] Roberts R, Kibler JJ. Mode-II fatigue crack propagation. J Basic Engng Series 1971;D93:671–80.
- [4] Tanaka K. Fatigue crack propagation from a crack inclined to the cyclic tensile axis. Eng Fract Mech 1974;6:493–507.
- [5] Sih GC. In: Sih GC, editor. A special theory of crack propagation in mechanics of fracture. Leyden: Noordhoff; 1973. p. XXI–XLV.

- [6] Sih GC. Fracture mechanics of engineering structural components. In: Sih GC, editor. Fracture mechanics methodology. The Hague: Martinus Nijhoff; 1984. p. 35–102.
- [7] Patel AB, Pandey RK. Fatigue crack growth under mixed-mode loading. *Fatigue Fract Eng Mater Struct* 1981;6:65–77.
- [8] Srinivas V, Vasudevan P. Studies of mixed-mode crack propagation in D16AT Al-alloy. *Engng Fract Mech* 1993;45(4):415–30.
- [9] Sander M, Richard HA. Finite element analysis of fatigue crack growth with interspersed mode I and mixed mode overloads. *Int J Fatigue* 2005;27:905–13.
- [10] Sander M, Richard HA. Experimental and numerical investigations on the influence of the loading direction on the fatigue crack growth. *Int J Fatigue* 2006;28:583–91.
- [11] Munro HG. The determination of fatigue crack growth rate by data smoothing technique. *Int J Fract* 1973;9(3):366–8.
- [12] Smith RA. The determination of Fatigue crack growth rate from experimental data. *Int J Fract* 1973;9(3):352–5.
- [13] Dinda Sudip, Daniel Kujawski. Correlation and prediction of fatigue crack growth for different R -ratios using K_{\max} and ΔK^+ parameters. *Eng Fract Mech* 2004;71:1779–90.
- [14] Sadananda K, Vasudevan AK. Crack tip driving forces and crack growth representation under fatigue. *Int J Fatigue* 2004;26:39–47.
- [15] Zhang J, He XD, Du SY. Analyses of the fatigue crack propagation process and stress ratio effects using the two parameter method. *Int J Fatigue* 2005;27:1314–8.
- [16] Richard HA. Fracture mechanical predictions for cracks with superimposed normal and shear loading. Dusseldorf: VDI-Verlag; 1985 (in German, in [9]).
- [17] Suresh S. Fatigue of materials. 1st ed. Cambridge University Press; 1992. p. 351.